Journal of Cellular Biochemistry 104:2248–2260 (2008)

PARP-1 Modulates Deferoxamine-Induced HIF-1α Accumulation Through the Regulation of Nitric Oxide and Oxidative Stress

Rubén Martínez-Romero,[1] Esther Martínez-Lara,[1] Rocío Aguilar-Quesada,[2] Andreína Peralta,[2] F. Javier Oliver,[2] and Eva Siles[1]*

[1]Department of Experimental Biology, University of Jaén, Paraje Las Lagunillas s/n, 23071-Jaén, Spain
[2]Institute of Parasitology and Biomedicine, CSIC, Granada, Spain

Abstract Poly(ADP-ribose) polymerase-1 (PARP-1) is a nuclear protein that, once activated by genotoxic agents, modulates the activity of several nuclear proteins including itself. Previous studies have established that PARP-1 inhibition may provide benefit in the treatment of different diseases, particularly those involving a hypoxic situation, in which an increased oxidative and nitrosative stress occurs. One of the most important transcription factors involved in the response to the hypoxic situation is the hypoxia-inducible factor-1 (HIF-1). The activity of HIF-1 is determined by the accumulation of its α subunit which is regulated, in part, by oxidative stress (ROS) and nitric oxide (NO), both of them highly dependent on PARP-1. Besides, HIF-1α can be induced by iron chelators such as deferoxamine (DFO). In this sense, the therapeutical use of DFO to strengthen the post-hypoxic response has recently been proposed. Taking into account the increasing interest and potential clinical applications of PARP inhibition and DFO treatment, we have evaluated the impact of PARP-1 on HIF-1α accumulation induced by treatment with DFO. Our results show that, in DFO treated cells, PARP-1 gene deletion or inhibition decreases HIF-1α accumulation. This lower HIF-1α stabilization is parallel to a decreased inducible NO synthase induction and NO production, a higher response of some antioxidant enzymes (particularly glutathione peroxidase and glutathione reductase) and a lower ROS level. Taken together, these results suggest that the absence of PARP-1 modulates HIF-1 accumulation by reducing both NO and oxidative stress. J. Cell. Biochem. 104: 2248–2260, 2008.

Key words: PARP-1; HIF-1α; deferoxamine; nitric oxide; oxidative stress

Poly(ADP-ribose) polymerase-1 (PARP-1) is a nuclear, zinc-finger, DNA-binding protein that detects specifically DNA-strand breaks generated by different genotoxic agents, such as ROS and peroxynitrite [D'Amours et al., 1999]. Once activated, it modulates the activity of different nuclear proteins, including itself, by catalysing the attachment of ADP-ribose units. Previous studies have established that PARP-1 inhibition may provide benefit in the treatment of different diseases, particularly those involving a hypoxic situation such as ischemia or cancer, in which an increased oxidative and nitrosative stress occurs [Eliasson et al., 1997; Zingarelli et al., 1997; Bowes and Thiemermann, 1998; Ding et al., 2001; Martin-Oliva et al., 2006]. Although the molecular mechanisms underlying this protection are not completely known, it has been reported that PARP-1 genetic ablation or pharmacological inhibition decreases the oxidative and nitrosative stress associated with those pathological situations [Oliver et al., 1999; Zingarelli et al., 2003; Cuzzocrea, 2005; Siles et al., 2005].

One of the most important transcription factors involved in the physiological responses to hypoxia is HIF-1, a heterodimeric DNA-binding complex composed of α and β subunits [Wang et al., 1995]. HIF-1β is constitutively expressed, so that HIF-1 activity depends on HIF-1α subunit level. In normoxic conditions, and with the presence of iron, HIF-1α is

Grant sponsor: Instituto de Salud Carlos III; Grant number: PI052020; Grant sponsor: Junta de Andalucía; Grant number: CVI-0184.

*Correspondence to: Eva Siles, Department of Experimental Biology, University of Jaén, Paraje Las Lagunillas s/n, 23071 Jaén, Spain. E-mail: esiles@ujaen.es

Received 5 November 2007; Accepted 12 March 2008
DOI 10.1002/jcb.21781

hydroxylated by HIF-1 prolyl hydroxylases (PHD), ubiquitinated by the von Hippel–Lindau protein and rapidly degraded by the proteosome [Epstein et al., 2001; Metzen et al., 2003a]. However, under hypoxic conditions or iron chelation, HIF-1α hydroxylation does not take place, its level is up-regulated, and consequently it can dimerize with the β subunit, creating the functional complex.

HIF-1α accumulation can be modulated by certain factors, such as oxidative and nitrosative stress, although their exact implication is controversial and probably linked [Kohl et al., 2006]. In this sense some authors have proposed that nitric oxide (NO) blocks HIF-1α stabilization [Sogawa et al., 1998; Agani et al., 2002; Hagen et al., 2003] while others contend that it causes HIF-1α accumulation [Brune and Zhou, 2003; Metzen et al., 2003b]. Similarly, ROS formation has also been linked to both HIF-1α induction and destabilization [Fandrey et al., 1994; Huang et al., 1996; Chandel et al., 2000; Kietzmann et al., 2000; Yang et al., 2003; Callapina et al., 2005a].

Iron chelators, such as deferoxamine (DFO), are widely used in the literature with two main different purposes. On the one hand, they are used as antioxidants as they prevent the iron from redox cycling and thereby inhibit hydroxyl formation by the Fenton or Haber–Weiss reaction [Williams et al., 1991; Saad et al., 2001]. However, and surprisingly, recent research has established that in certain situations DFO may also increase the oxidative status by decreasing the GSH cellular level [Seo et al., 2006] or inducing reactive oxygen species (ROS) production [Cadenas and Davies, 2000]. On the other hand, iron chelators are also used as a hypoxic-mimetic agent as they have been shown to mimic the effect of oxygen deprivation by inducing a number of hypoxia-response genes [Gleadle and Ratcliffe, 1998; Bianchi et al., 1999; Zhu and Bunn, 1999]. Based on this background, some authors have proposed the therapeutical use of DFO to ameliorate the hypoxic damage or to strengthen the post-hypoxic response [Palmer et al., 1994; Hurn et al., 1995; Groenendaal et al., 2000; Mu et al., 2005; Freret et al., 2006].

Taking into account the involvement of both NO and ROS in the activation of HIF-1α, and considering that both parameters are regulated by PARP-1 (both by the protein and the activity), we propose to evaluate the impact of PARP-1 on HIF-1α accumulation by DFO treatment.

MATERIALS AND METHODS

Cell Culture and Treatments

Immortalized murine embryonic fibroblasts (MEFs) and primary MEFs derived from day-13.5 embryos, expressing or lacking PARP-1 (*parp-1*$^{+/+}$ *and parp-1*$^{-/-}$), were grown in 10% foetal bovine serum supplemented Dulbecco's modified Eagle's medium (FBS–DMEM, Sigma, St. Louis, MO, USA) and incubated at 37°C in a humidified atmosphere of 5% O_2, 5% CO_2, and 90% N_2. Fibroblasts were treated for different periods of time with the iron chelator deferoxamine DFO at a subcytotoxic dose (200 μM). The PARP inhibitor 3,4-dihydro-5-[4-(1-piperidinyl)butoxyl]-1(2H)-isoquinolinone (DPQ; Alexis Biochemicals, San Diego, CA; 40 μM), dissolved in culture medium immediately before use, was employed to corroborate the results obtained in *parp-1* knockout cells. DPQ solutions also contained <1% DMSO to improve solubility as it is sparingly soluble in water. When used, DPQ was added simultaneously to DFO and thereafter present in the culture throughout the experiment.

Western Blot

For Western blot analysis, equal amounts of denatured total-protein extracts were loaded and separated in 7.5% or 12% SDS-polyacrylamide gel (HIF-1α and Mn-SOD, respectively). Proteins in the gel were transferred to a PVDF membrane (Amersham Pharmacia Biotech, Buckinghamshire, UK) and then blocked. Polyclonal antibodies to HIF-1α (1/1000, Bethyl Lab, Inc., Montgomery, TX) and Mn-SOD (1/8000, StressGen Biotechnologies Corp., Victoria B.C., Canada) and a monoclonal antibody to α-tubulin (Sigma, St. Louis, MO, USA), as internal control, were used for detection of the respective proteins. Antibody reaction was revealed with chemiluminescence detection procedures according to the manufacturer's recommendations (ECL kit, Amersham Corp., Buckinghamshire, UK).

Real-Time RT-PCR

Gene expression of adrenomedullin (AM) was quantitatively assessed by real-time PCR using β-actin as the normalizing gene. Total RNA was isolated from cell extracts using TRIzol reagent

(Invitrogen) according to the manufacturer's instructions. After treating with DNase, cDNA was synthesized from 1.5 μg total RNA using reverse transcriptase (SuperscriptTM III RT, Invitrogen) with oligo-(dT) 15 primers (Promega). Real-time PCR was performed on the Stratagene MxPro 3005P qPCR system using the DyNAmo HS SYBR Green qPCR kit (Finnzymes, Espoo, Finland). Nucleotide sequences of the primers were as follows: 5′-CAGCAATCAGAGCGAAGC-3′ (forward) and 5′-ATGCCGTCCTTGTCTTTGTC-3′ (reverse) for AM; 5′-TGAGGAGCACCCTGTGCT-3′ (forward) and 5′-CCAGAGGCATACAGGGAC-3′ (reverse) for β-actin. Experiments were performed with triplicates, and the values were used to calculate the ratio of AM to β-actin, with a value of 1 used as the control.

PARP Activity Assay

PARP activity after DFO treatment was assayed, in wild-type cells, using a colorimetric kit according to the manufacturer's instructions (Universal Colorimetric PARP Assay Kit with Histone-Coated Strip Wells, Trevigen).

NO Measurement

Nitric oxide (NO) production was indirectly quantified by determining nitrate/nitrite and *S*-nitroso compounds (NO_x), using an ozone chemiluminescence-based method. For an estimation of the NO_x level, at the end of each treatment time, cells were collected and lysed by three freeze–thaw cycles. After centrifugation at 14,000*g* for 30 min, supernatants were collected and protein was quantified [Bradford, 1976]. Samples were deproteinized in deproteinization solution (0.8N NaOH and 16% $ZnSO_4$). The total amount of NO_x in the deproteinized samples was determined by a modification [López-Ramos et al., 2005] of the procedure described by Braman and Hendrix [1989] using the purge system of Sievers Instruments, model NOA 280i. NO_x concentrations were calculated by comparison with standard solutions of sodium nitrate. Final NO_x values were referred to the total protein concentration in the initial extracts.

iNOS Confocal Microscopy

The iNOS expression was evaluated by confocal microscopy. Briefly, cells were grown on slides and treated for 24 h either with DFO (*parp-1*$^{+/+}$ and *parp-1*$^{-/-}$) or DFO+DPQ (*parp-1*$^{+/+}$). Afterwards, cells were washed three times in PBS, fixed in fresh cold 4% paraformaldehyde for 10 min, washed again with PBS, permeabilized with PBS/0.2% Triton X-100 for 5 min, and blocked with 5% bovine serum albumin. Cells were incubated o/n at 4°C with iNOS monoclonal antibody (1/100 in PBS/0.2% Triton X-100 and 1% bovine serum albumin; Transduction Lab., Lexington, KY) and then washed three times in PBS/0.2% Triton X-100. The secondary antibody, linked to the Cy2, was diluted 1/1000 in PBS/0.2% Triton X-100 and incubated for 2 h at room temperature in the dark. Finally cells were washed three times in PBS/0.2% Triton X-100 and stained with DRAF 5 (1/2500) for 15 min. After mounting, slides were coverslipped and stored in the dark at 4°C. Results were compared with those found in control cells.

Measurement of Intracellular Generation of ROS

Flow-cytometric analysis of the intracellular generation of ROS was performed using 2′, 7′-dichlorofluorescein diacetate (DCFH) as a probe. ROS in the cells oxidize DCFH, yielding highly fluorescent 2′,7′-dichlorofluorescein (DCF). Cells were cultured in six-well plates and treated with DFO (200 μM) for different experimental times. One hour before the end of the experiment, DCFH (2 μg/ml) was added. Once the incubation was finished, cells were harvested, washed, centrifuged, resuspended in DMEM medium, and analysed by flow cytometry (excitation at 504 nm and fluorescence detection at 530 nm). Fluorescence was analysed in viable cells characterized by forward scatter *versus* side scatter. Data were normalized to the control values.

ROS production was also evaluated by confocal microscopy. Briefly, cells were grown on slides and treated for 24 h either with DFO (*parp-1*$^{+/+}$ and *parp-1*$^{-/-}$) or DFO+DPQ (*parp-1*$^{+/+}$). One hour before the end of the experiment DCFH (2 μg/ml) was added. Afterwards, cells were washed three times in PBS, fixed in fresh cold 4% paraformaldehyde for 10 min, washed again with PBS and stained with DRAF 5 (1/2500) for 15 min. After mounting, slides were coverslipped and stored in the dark at 4°C. Results were compared with control.

Antioxidant Enzyme Assays

At the end of each incubation period, cells were collected, washed with cold PBS and lysed

for 20 min at 4°C in EBC buffer (20 mM Tris–HCl pH 8; 150 mM NaCl, 1 mM EDTA, 0.5% NP-40) with protease inhibitors. After centrifugation at 14,000*g* for 15 min at 4°C, supernatants were collected and protein was quantified [Bradford, 1976].

Glutathione transferase (GST) activity towards the 1-chloro-2,4-dinitrobenzene (CDNB) was measured spectrophotometrically, as described by Habig et al. [1974]. Catalase (CAT) activity was studied by monitoring the decomposition of H_2O_2 at 240 nm, according to the method described by Beers and Sizer [1952]. Glutathione reductase (GR) activity was measured by following the rate of NADPH oxidation at 340 nm [Carlberg and Mannervik, 1985]. Superoxide dismutase (SOD) activity was assayed by measuring the rate of inhibition of cytochrome *c* reduction by superoxide anions generated by a xanthine/xanthine oxidase system [Flohé and Ötting, 1984]. As a means of discriminating between Cu/Zn-SOD and Mn-SOD activities, the assay was additionally performed after incubation in the presence of KCN, which selectively inhibits Cu/Zn-SOD isoform. Glutathione peroxidase (GPX) activity was determined in a coupled assay with GR using H_2O_2 as a substrate [Flohé and Günzler, 1984].

Statistical Analysis

Data are expressed as means ± S.D. Statistical comparisons between the different experimental times of DFO treated *parp-1*$^{-/-}$ and *parp-1*$^{+/+}$ cells and their corresponding controls were made by one-way ANOVA with a *post hoc* Student's *t*-test, accepting $P < 0.05$ as the level of significance. The effect of PARP-1 was evaluated by a two-way ANOVA followed by a *post hoc* Student's *t*-test.

RESULTS

HIF-1α Stabilization is Modulated by PARP-1

To investigate the effect of PARP-1 on DFO-mediated HIF-1α stabilization, we monitored the amount of this transcription factor in wild-type and *parp-1*$^{-/-}$ immortalised MEFs. As shown in Figure 1a, after 24 h of treatment HIF-1α was significantly more expressed in DFO-treated wild-type cells than in their counterpart *parp-1*$^{-/-}$. This result was corroborated in primary *parp-1*$^{+/+}$ and *parp-1*$^{-/-}$ MEFs (Fig. 1b). Moreover, the pharmacological inhibition of PARP in wild-type cells also decreased HIF-1α induction after DFO treatment (Fig. 1c).

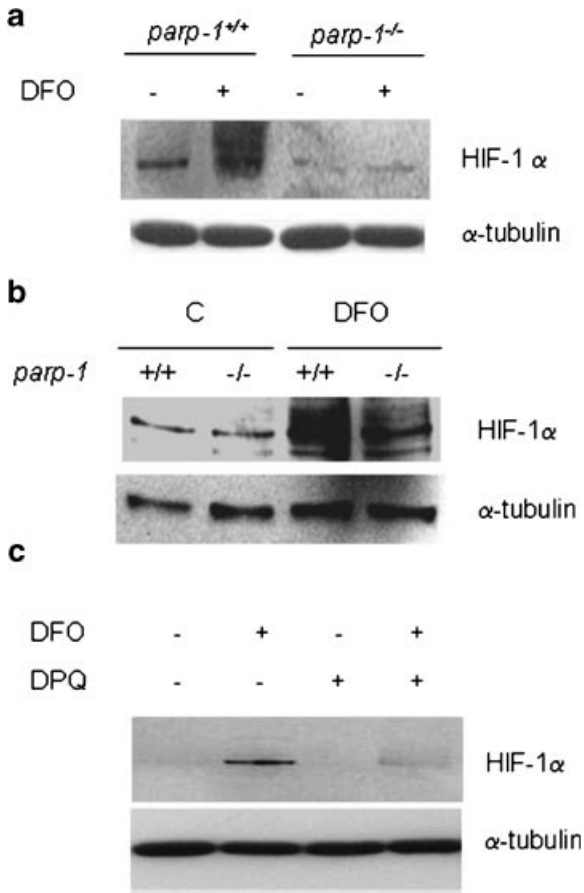

Fig. 1. Western blot analysis of the effect of PARP-1 on DFO-mediated HIF-1α stabilization after 24 h of treatment. Representative immunoblot of HIF-1α expression in control and DFO-treated wild-type and *parp-1*$^{-/-}$ immortalised **(a)** or primary **(b)** MEFs. **(c)** Representative Western blot of HIF-1α expression in control and DFO-treated wild-type cells in the presence or absence of the PARP inhibitor DPQ. α-Tubulin immunodetection was also included as a protein-loading control.

To analyze HIF-1 activation in response to DFO we observed the transcription of the typical HIF-1 target gene AM [Garayoa et al., 2000]. The real-time PCR results (Fig. 2) show that the expression of AM is greatly influenced by the presence of PARP-1. Particularly, after 24 h of DFO treatment AM mRNA levels were significantly higher in *parp-1*$^{+/+}$ cells.

Altogether, these results suggest a role of PARP-1 in HIF-1α accumulation and activity.

The Absence of PARP-1 Promotes an Altered NO Response

NO is a free radical reportedly involved in HIF-1α stabilization. In our experimental model, the absence of PARP-1 induced altered NO production, which could be linked to the

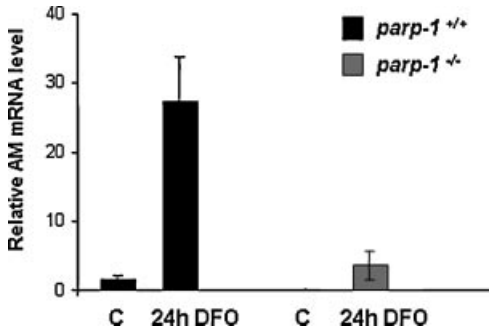

Fig. 2. Effect of DFO treatment on AM mRNA expression in *parp-1*$^{+/+}$ and *parp-1*$^{-/-}$ cells. The results are expressed as mRNA expression relative to control wild-type cells after normalization against beta-actin. Each sample was analysed in triplicate. The mean ± SD of three RNA extracts for each experimental condition is represented.

differential HIF-1α accumulation previously observed in *parp-1*$^{+/+}$ and *parp-1*$^{-/-}$ *cells*.

As shown in Figure 3a, basal NO_x level in control cells was significantly decreased in *parp-1*$^{-/-}$ cells ($P < 0.001$). Moreover, the absence of PARP-1 promoted a different NO response to DFO ($P < 0.02$). Particularly, in wild-type cells the treatment induced an initial decrease in the NO_x level, which was followed by the recovery of the basal level (12 and 16 h) and a sharp increase ($P < 0.001$) after 24 h of treatment. In the absence of PARP-1, this rise also occurred, but was considerably lower than in *parp-1*$^{+/+}$ cells.

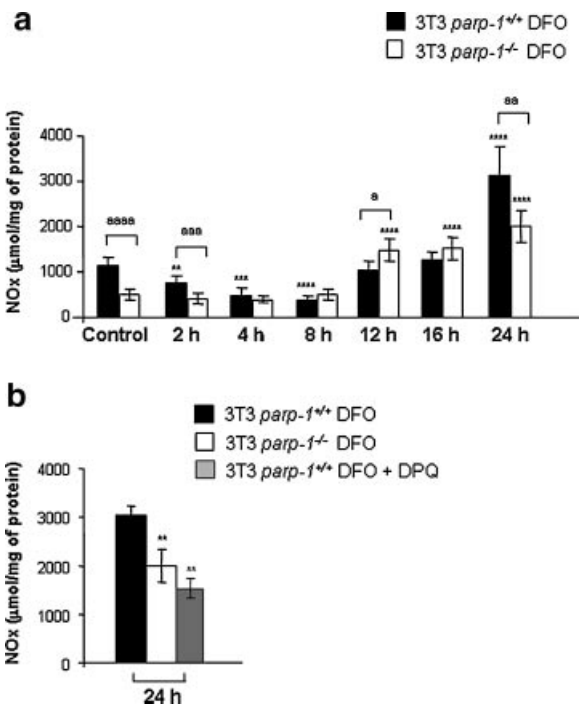

Fig. 3. **a**: Effect of DFO treatment on NOx levels (µmol/mg of protein) in *parp-1*$^{+/+}$ and *parp-1*$^{-/-}$ cells. **b**: NOx levels in *parp-1*$^{+/+}$, *parp-1*$^{-/-}$ and PARP inhibited cells (DPQ) after 24 h of DFO treatment. Values represent the mean ± SD from three independent experiments. Statistically significant differences from the corresponding control group: $^{**}p < 0.02$; $^{***}p < 0.01$ and $^{****}p < 0.001$. Statistically significant differences between *parp-1*$^{+/+}$ and *parp-1*$^{-/-}$ cells: $^{a}p < 0.05$, $^{aa}p < 0.02$, $^{aaa}p < 0.01$, and $^{aaaa}p < 0.001$.

To confirm the involvement of PARP-1 on NO production, we cotreated wild-type cells with DFO and with the PARP inhibitor DPQ for 24 h. Our results (Fig. 3b) showed that the NO peak detected in wild-type cells after a 24 h treatment was significantly lowered by inhibiting PARP ($P < 0.02$). Moreover, the NO production in PARP inhibited cells reproduced that found in *parp-1*$^{-/-}$ cells. These results strongly suggest that PARP-1 is related to the final NO burst observed in wild-type cells.

DFO-Induced iNOS Expression is Decreased in PARP-1 Null Cells and after PARP Inhibition

Although NO can be generated by different mechanism, the sharp increase of NO detected in wild-type cells after 24 h of DFO treatment seemed to indicate the implication of the iNOS isoform. Consequently we analysed, after this time, the iNOS expression by confocal microscopy in both *parp-1*$^{+/+}$ and *parp-1*$^{-/-}$ cell lines and in PARP inhibited cells. As reflected in Figure 4, iNOS level was considerably higher in wild-type cells and the inhibition of PARP mimicked the expression observed in *parp-1* knock-out cells.

DFO Induces ROS Production only in the Presence of PARP-1

Oxidative stress seems to be one of the factors involved in HIF-1α stabilization. Moreover, it is known that PARP-1 presence induces a higher oxidative status in cells [Groenendaal et al., 2000; Zhou et al., 2006]. To test whether, in our experimental model, PARP-1 affected the oxidative status, we next analysed ROS levels before and after DFO treatment in wild-type and *parp-1* knock-out cells (Fig. 5). The results (Fig. 5a) demonstrate that ROS production significantly differed in the two cell lines ($P < 0.001$) after treatment. In fact, although a progressive increase in ROS production, which became significant after 12 h ($P < 0.05$), was observed in wild type cells, no changes were detected in the *parp-1*$^{-/-}$ ones. PARP-1 involvement in oxidative stress generation was confirmed by simultaneously treating

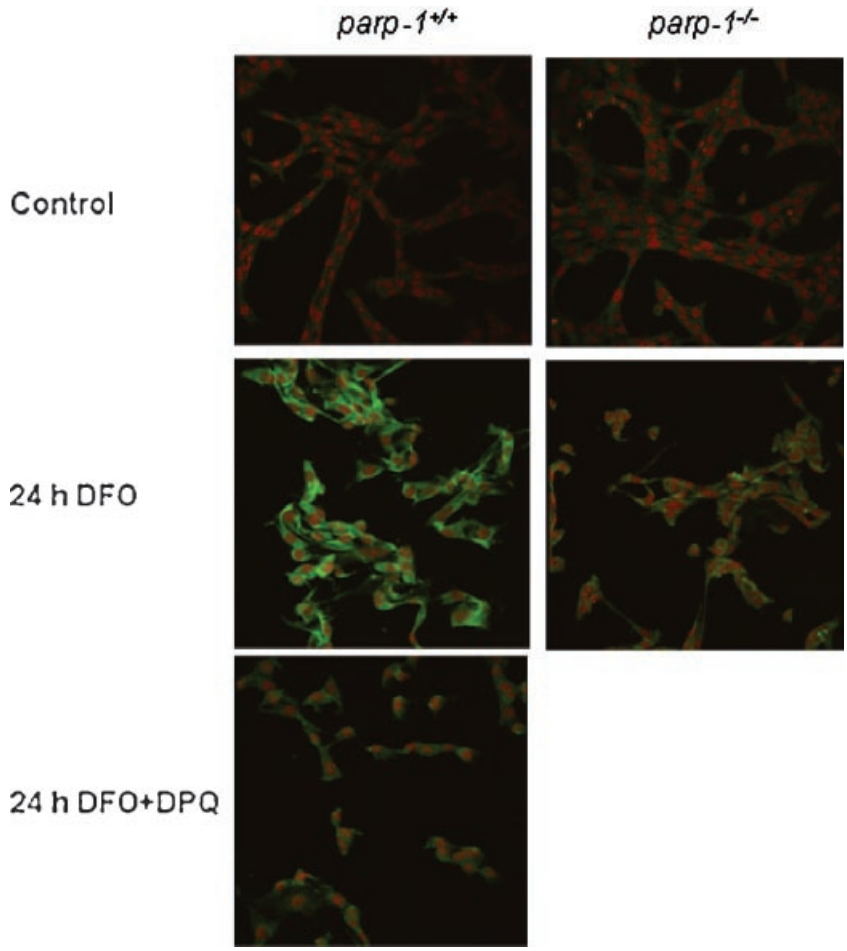

Fig. 4. Confocal immunofluorescence of iNOS in *parp-1*$^{+/+}$, DPQ-treated, and *parp-1*$^{-/-}$ cells after 24 h of DFO exposure. Control cells of the two different genotypes are also shown.

wild-type cells with DFO and DPQ for 24 h, the experimental time in which the oxidative stress was highest. As shown in Figure 5b, PARP-1 inhibition significantly prevented ROS production. These results by flow cytometry were confirmed by confocal microscopy (Fig. 6). Therefore, we conclude that PARP-1 involves higher oxidative stress after DFO treatment.

PARP-1 Activity is Induced after DFO Treatment

Genotoxic agents, such as ROS, induce PARP-1 activation [D'Amours et al., 1999]. Considering the effect of the presence of PARP-1 on ROS production, we evaluated whether DFO treatment induced PARP activity. We chose the 16 and 24 h experimental times in which a patent ROS increase had been previously observed only in wild-type cells. The results shown in Figure 7 revealed a significant PARP activation after DFO treatment ($P < 0.05$).

Mn-SOD is Differently Expressed in *parp-1*$^{+/+}$ and *parp-1*$^{-/-}$ Cells

ROS are produced mainly in mitochondria. Mn-SOD, due to its mitochondrial location, represents an important initial component in the cellular defence against ROS. In this context, we hypothesized that DFO treatment may induce a different Mn-SOD level in *parp-1*$^{+/+}$ *and parp-1*$^{-/-}$ cells. As shown in Figure 8, Mn-SOD expression was clearly higher in wild-type cells, although no changes were detected after treatment in any of the cell lines.

Parp-1 Abrogation Decreases the Activity of the Main Antioxidative Enzymes but Allows a Higher Antioxidant Response after the Treatment

Finally, to complete the overall view of the oxidative status, we tested the activity of

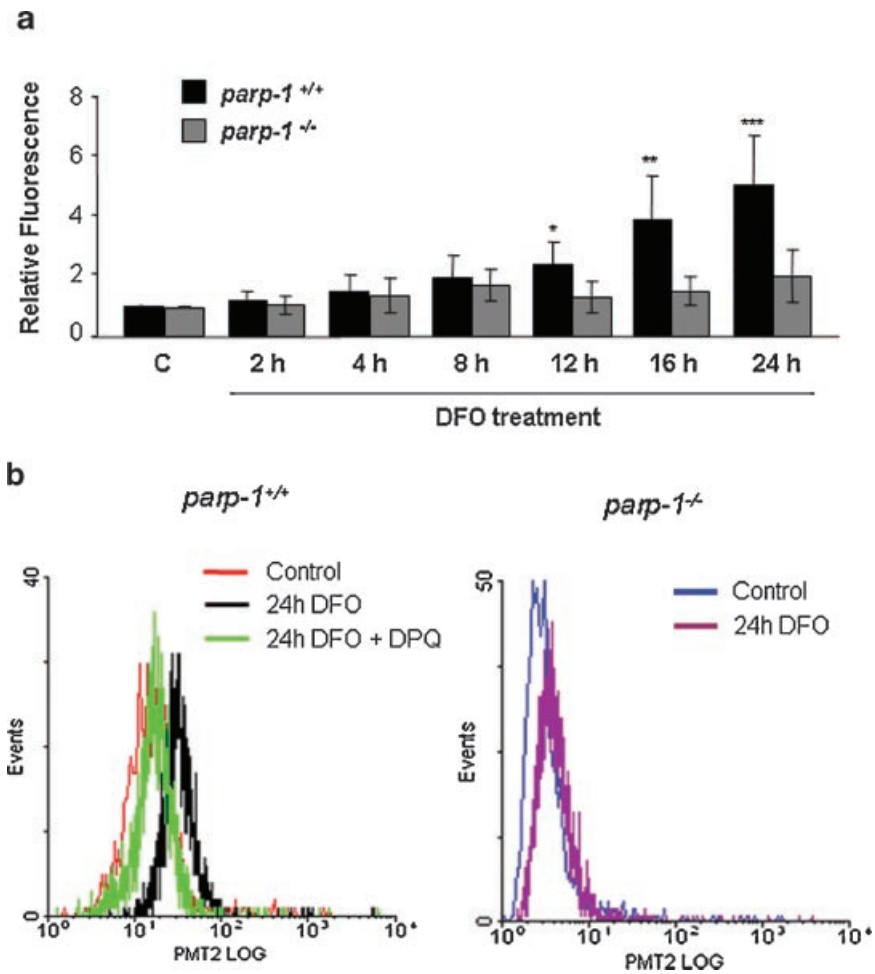

Fig. 5. **a**: Time course of ROS generation in DFO-treated cells. DCF fluorescence as a measurement of ROS production was determined by flow cytometry. Mean values of the log fluorescence for *parp-1*$^{+/+}$ and *parp-1*$^{-/-}$ cells at different times after DFO treatment. Results were normalized to those in control cells in the different genotypes. Values are given as the means ± SD from three independent experiments. Statistically significant differences from the corresponding control group: $^{*}p < 0.05$, $^{**}p < 0.02$ and $^{***}p < 0.01$. **b**: Effect of pharmacological PARP inhibition on ROS production after DFO treatment. The increased ROS level observed in *parp-1*$^{+/+}$ cells after a 24 h DFO incubation was reduced by co-treatment with DPQ. Representative traces displayed by flow cytometry in *parp-1*$^{+/+}$ cells, with and without DPQ, and in *parp-1*$^{-/-}$ cells after 24 h of DFO treatment are shown. Results for control cells are also displayed.

the main antioxidant enzymes (GST, CAT, GR, Mn-SOD, Cu/Zn-SOD, GPX) in the presence or absence of PARP-1 (Fig. 9). PARP-1 presence sharply boosted the basal activity of all the enzymes assayed. However, DFO treatment in wild-type cells promoted no further rise in any of the enzymatic activities analysed. Moreover, Cu/Zn-SOD activity even decreased after 16 and 24 h, in parallel with the augment in the ROS production previously described. On the contrary, in *parp-1*$^{-/-}$ cells, a significant increase was observed in Cu/Zn-SOD after 8 h and in Se-GPX and GR activity after 8, 12, and 16 h of DFO treatment.

DISCUSSION

DFO is an iron chelator which has been shown to ameliorate the damage induced by hypoxia-ischemia [Palmer et al., 1994; Hurn et al., 1995; Groenendaal et al., 2000; Mu et al., 2005; Freret et al., 2006]. One of the mechanisms proposed for its therapeutical use is the induction of HIF-1α accumulation, a transcription factor involved in the expression of several genes that facilitate the adaptation to hypoxia, in which PARP-1 activation appears to play a pivotal role. The activity of the transcription factor HIF-1 seems to be regulated by different factors

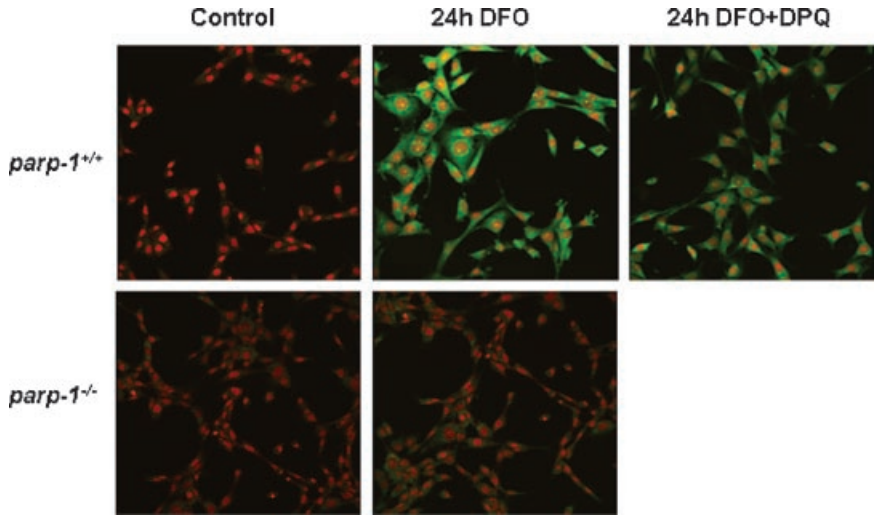

Fig. 6. Confocal immunofluorescence of DCF fluorescence in *parp-1*$^{+/+}$ cells, with and without DPQ, and in *parp-1*$^{-/-}$ cells after 24 h of DFO treatment. Photographs of cells without treatment are also shown.

such as ROS and NO, both related to PARP-1. Taking into account the increasing interest and potential clinical applications of PARP inhibition and DFO treatment, and considering the pathophysiological role of ROS and NO, we have analysed the effect of PARP-1 on HIF-1α accumulation induced by DFO.

Our results show that in DFO-treated cells, PARP-1 gene deletion or inhibition decreases HIF-1α accumulation. This deficient HIF-1α stabilization is parallel to a decreased oxidative stress, iNOS induction and NO production, suggesting that PARP-1 absence modulates HIF-1 accumulation by reducing both ROS and NO level (Fig. 10).

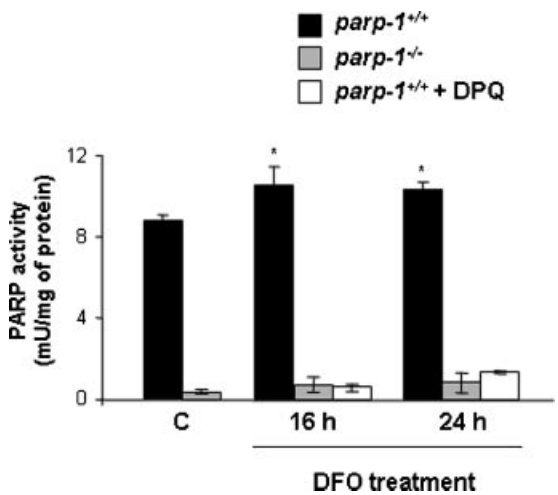

Fig. 7. PARP activity in control, 16 and 24 h DFO-treated *parp-1*$^{+/+}$ and *parp-1*$^{-/-}$ cells. Data obtained in DPQ+DFO (16 and 24 h) *parp-1*$^{+/+}$ cells are also included. Values represent mean ± SD from three independent experiments. Unit definition: 1 U PARP incorporates 100 pmol poly(ADP) from NAD^+ into acid-insoluble form in 1 min at 22°C. Statistically significant differences from the control group: $^*p < 0.05$.

Inhibition of PHD through iron chelation is recognized as the main mechanism responsible for the stabilization of HIF-1α after DFO treatment. However, ROS have also been proposed as signalling molecules which take part in HIF-1α regulation, and, vice versa, HIF-1α induction has also been associated with the protection of cells against certain forms of oxidative stress [Zaman et al., 1999; Siren et al., 2000; Digicaylioglu and Lipton, 2001]. Concerning the first point, some authors have proposed that ROS production decreases HIF-1α accumulation probably by restoring PHD activity, favouring HIF-1α degradation [Huang et al., 1996; Callapina et al., 2005a]. However, according to our results, others suggest that free radicals mediate HIF-1α accumulation [Chandel et al., 1998; Agani et al., 2000; Quintero et al., 2006]. In this sense, the results presented here show that a higher HIF-1α accumulation is observed only in those cells (*parp-1*$^{+/+}$) in which ROS production after DFO treatment steadily increases. Moreover the implication of PARP-1 in this process is corroborated by the results obtained in *parp-1* deleted cells or after PARP inhibition.

Oxidative stress can be generated by the rise in ROS formation, by the restricted/insufficient antioxidative defence mechanisms or by the combination of the two. The analysis of the main

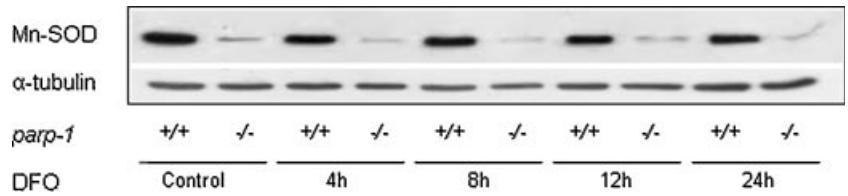

Fig. 8. Analysis of Mn-SOD expression in control and DFO-treated *parp-1*$^{+/+}$ and *parp-1*$^{-/-}$ cells. A representative immunoblot is shown. α-tubulin immunodetection was also included as a protein-loading control.

antioxidant enzymes revealed that the higher ROS level found in wild-type cells is concomitant to a higher antioxidant activity, suggesting a cellular adaptation to ROS. In addition, we have demonstrated that Mn-SOD, a mitochondrial enzyme which scavenges superoxide and converts it to H_2O_2, is significantly more expressed in wild-type cells. In this sense, it has been published that exposure to low ROS concentrations may act as a preconditioning factor which induces the enzymatic antioxidant system [Ravati et al., 2000]. In fact, the lower oxidative stress in cells with PARP-1 genetic deletion correlates with a lower, but quite efficient, activity of the main antioxidant enzymes. The role of DFO on oxidative stress is somewhat controversial, however its effect on the antioxidative enzymes

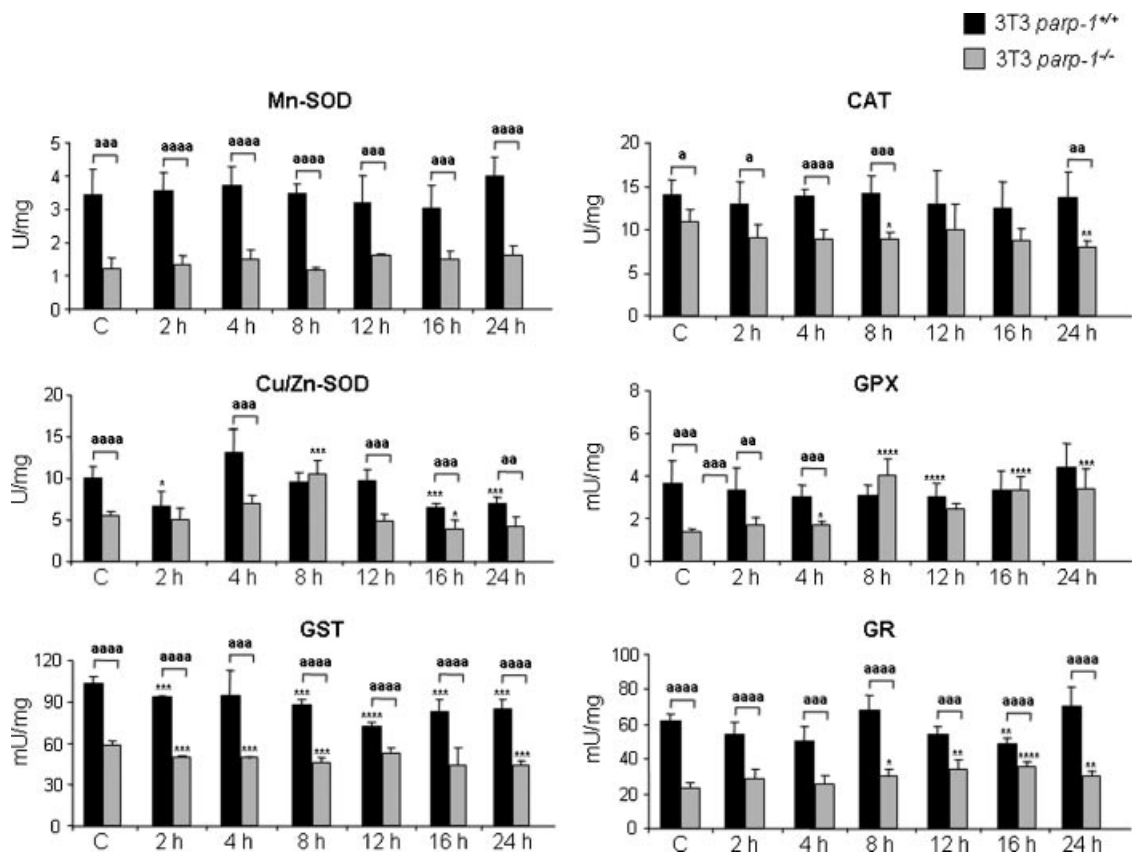

Fig. 9. Effect of DFO treatment on Mn-SOD, Cu/Zn-SOD, GST, CAT, GPX and GR activity. Data are expressed as mean ± SD for n = 4 per group in U/mg or mU/mg of protein. One SOD unit is defined as the amount of enzyme that inhibits the rate of cytochrome *c* reduction by 50%. One unit of GST activity is defined as the amount of enzyme needed to form 1 μmol of GSH-CDNB conjugate per min. One CAT unit is defined as the amount of enzyme that catalyses the decomposition of 1 μmol of H_2O_2 per min. One unit of GPX or GR activity is defined as the amount of enzyme that catalyses the oxidation of 1 μmol of NADPH per min. Statistically significant differences from the corresponding control group: $^{*}p < 0.05$, $^{**}p < 0.02$, $^{***}p < 0.01$, $^{****}p < 0.001$. Statistically significant differences between *parp-1*$^{+/+}$ and *parp-1*$^{-/-}$ cells: $^{a}p < 0.05$, $^{aa}p < 0.02$, $^{aaa}p < 0.01$ and $^{aaaa}p < 0.001$.

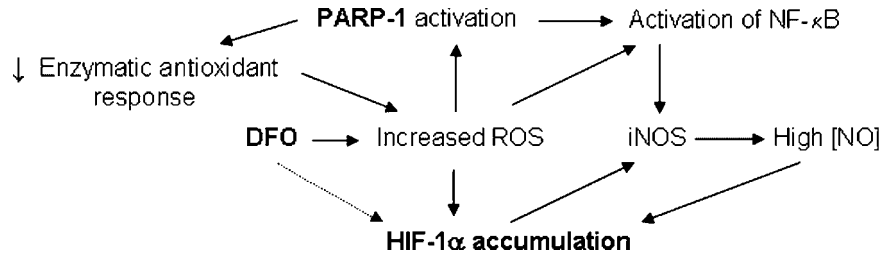

Fig. 10. Proposed model of action of PARP-1 in DFO-induced HIF-1α accumulation. DFO induces HIF-1α accumulation directly (. . .) or indirectly (—). PARP-1 plays a pivotal role, through its effect on ROS and NO production, in the indirect pathway. For details, please see the text.

is very weak [Kadikoylu et al., 2004]. In agreement with those findings, we have observed no increased enzymatic antioxidant activity after DFO treatment in wild-type cells, but a decrease in Cu/Zn-SOD at the end of the experiment, which correlates with the higher ROS production. However *parp-1* deletion favours the response of some enzymes, particularly GPX and GR. GR is important for the maintenance of GSH level which is used by other antioxidant systems, such as the GPX. These results appear to indicate that, although it has been proposed that DFO may increase the oxidative status by reducing GSH cellular level [Seo et al., 2006], the absence of PARP-1 ameliorates this effect. Moreover, it has been reported that the activity of Mn-SOD affects HIF-1α accumulation [Huang et al., 1996; Wang et al., 2005]. In our experimental model, Mn-SOD activity and expression is considerably reduced in *parp-1*-deleted cells. However, the fact that neither the activity nor the expression of this enzyme is affected by DFO, independently of PARP-1 presence, makes it difficult to establish a relationship between Mn-SOD and HIF-1α induction.

NO is a free radical which has also been shown to play a role on the stabilization of HIF-1α [Callapina et al., 2005a; Callapina et al., 2005b; Kohl et al., 2006; Quintero et al., 2006; Berchner-Pfannschmidt et al., 2007]. In this sense, we have observed that, according to the HIF-1α results, DFO treatment induced a different NO response in wild-type and PARP inhibited or PARP-1 null cells. NO has been described either to inhibit or to enhance HIF-1α accumulation depending on the experimental conditions. It has been proposed that under normoxic conditions, such as those in DFO-treated cells, NO inhibits PHD activity, inducing HIF-1α stabilization by competing for O_2 at the central iron of the active site [Zhang et al., 2002; Quintero et al., 2006]. In our study, the higher HIF-1α accumulation detected in *parp-1*$^{+/+}$ cells points to a link between higher NO levels and the HIF-1α induction. In fact, we have demonstrated that, in those cells and in the same experimental conditions, an ameliorated NO increase achieved by co-treatment with a PARP inhibitor coincides with a lower HIF-1α induction. This result argues in favour of both the implication of PARP-1 in NO production and the importance of NO on HIF-1α accumulation, suggesting that PARP-1 inhibition, by a slight induction of NO, decreases DFO-induced HIF-1α accumulation.

Iron chelators, such as DFO, can reportedly induce transcription of iNOS [Weiss et al., 1994; Dlaska and Weiss, 1999], although this effect does not always occur [Woo et al., 2006]. The sharp increase of NO detected in wild-type cells after 24 h of DFO treatment pointed to the induction of iNOS, the isoform which generates the highest concentrations of NO and which, in turn, is up-regulated by HIF-1 [Palmer et al., 1998; Semenza, 2005]. In fact, we have observed that the DFO treatment induced iNOS expression, although the response was quantitatively reduced after genetic deletion of PARP-1. In this sense, it is well known that PARP-1 is a co-modulator of NF-κB, and PARP-1-deficient cells and mice display reduced iNOS induction [Oliver et al., 1999; Conde et al., 2001]. Moreover, it is known that ROS, and especially O_2^-, are major modulators of NO activity [Grisham et al., 1999]. In this context, it can be assumed that the increased ROS production observed in wild-type cells after DFO treatment could enhance NF-κB activation [Schreck et al., 1991], promoting iNOS induction and the consequent final burst in NO production detected in these cells. Moreover, the increased HIF-1α accumulation observed particularly in *parp-1*$^{+/+}$ cells may also cooperate in the

induction of iNOS. Finally, as we have shown that DFO treatment activated PARP-1, it can be assumed that both DFO and PARP-1 activation cooperate, through iNOS induction, to prompt the final rise in NO production detected in wild-type cells.

In conclusion, the data presented here and summarized in Figure 10, suggest that PARP-1 inhibition decreases DFO-induced HIF-1α accumulation by modulating the NO level and by decreasing oxidative stress.

ACKNOWLEDGMENTS

We first wish to thank Mr. Ricardo Oya for his excellent technical assistance, and Mr. David Nesbitt for his editorial help. This work was supported by the Instituto de Salud Carlos III (PI052020) and the Junta de Andalucía (CVI-0184).

REFERENCES

Agani FH, Pichiule P, Chavez JC, LaManna JC. 2000. The role of mitochondria in the regulation of hypoxia-inducible factor 1 expression during hypoxia. J Biol Chem 275:35863–35867.

Agani FH, Puchowicz M, Chavez JC, Pichiule P, LaManna J. 2002. Role of nitric oxide in the regulation of HIF-1alpha expression during hypoxia. Am J Physiol 283: C178–C186.

Beers KF Jr, Sizer IW. 1952. A spectrophotometric method of measuring the breakdown of hydrogen peroxide by catalase. J Biol Chem 195:133–139.

Berchner-Pfannschmidt U, Yamac H, Trinidad B, Fandrey J. 2007. Nitric oxide modulates oxygen sensing by hypoxia-inducible factor 1-dependent induction of prolyl hydroxylase. J Biol Chem 282:1788–1796.

Bianchi L, Tacchini L, Cairo G. 1999. HIF-1-mediated activation of transferrin receptor gene transcription by iron chelation. Nucleic Acids Res 21:4223–4227.

Bowes J, Thiemermann C. 1998. Effects of inhibitors of the activity of poly (ADP-ribose) synthetase on the liver injury caused by ischaemia-reperfusion: a comparison with radical scavengers. Br J Pharmacol 124:1254–1260.

Bradford MM. 1976. A rapid and sensitive method for the quantification of microgram quantities of protein utilizing the principle of protein-dye binding. Anal Biochem 72:248–254.

Braman RS, Hendrix SA. 1989. Nanogram nitrite and nitrate determination in environmental and biological materials by vanadium (III) reduction with chemiluminescence detection. Anal Chem 61:2715–2718.

Brune B, Zhou J. 2003. The role of nitric oxide (NO) in stability regulation of hypoxia inducible factor-1alpha (HIF-1alpha). Curr Med Chem 10:845–855.

Cadenas E, Davies KJ. 2000. Mitochondrial free radical generation, oxidative stress, and aging. Free Radic Biol Med 29:222–230.

Callapina M, Zhou J, Schmid T, Kohl R, Brune B. 2005a. NO restores HIF-1alpha hydroxylation during hypoxia: role of reactive oxygen species. Free Radic Biol Med 39: 925–936.

Callapina M, Zhou J, Schnitzer S, Metzen E, Lohr C, Deitmer JW, Brune B. 2005b. Nitric oxide reverses desferrioxamine- and hypoxia-evoked HIF-1alpha accumulation–implications for prolyl hydroxylase activity and iron. Exp Cell Res 306:274–284.

Carlberg I, Mannervik B. 1985. Glutathione reductase. Methods Enzymol 113:484–499.

Chandel NS, Maltepe E, Goldwasser E, Mathieu CE, Simon MC, Schumacker PT. 1998. Mitochondrial reactive oxygen species trigger hypoxia-induced transcription. Proc Natl Acad Sci USA 95:11715–11720.

Chandel NS, McClintock DS, Feliciano CE, Wood TM, Melendez JA, Rodriguez AM, Schumacker PT. 2000. Reactive oxygen species generated at mitochondrial complex III stabilize hypoxia-inducible factor-1alpha during hypoxia: a mechanism of O_2 sensing. J Biol Chem 275:25130–25138.

Conde C, Mark M, Oliver FJ, Huber A, de Murcia G, Menissier-de Murcia J. 2001. Loss of poly(ADP-ribose) polymerase-1 causes increased tumour latency in p53-deficient mice. EMBO J 20:3535–3543.

Cuzzocrea S. 2005. Shock, inflammation and PAR. Pharmacol Res 52:72–82.

D'Amours D, Desnoyers S, D'Silva I, Poirier GG. 1999. Poly(ADP-ribosyl)ation reactions in the regulation of nuclear functions. Biochem J 342:249–268.

Digicaylioglu M, Lipton SA. 2001. Erythropoetin-mediated neuroprotection involves cross talk between Jak2 and NF-κB signalling cascades. Nature 412:641–647.

Ding Y, Zhou Y, Lai Q, Li J, Gordon V, Diaz FG. 2001. Long-term neuroprotective effect of inhibiting poly(ADP-ribose) polymerase in rats with middle cerebral artery occlusion using a behavioral assessment. Brain Res 915: 210–217.

Dlaska M, Weiss G. 1999. Central role of transcription factor NF-IL6 for cytokine and iron-mediated regulation of murine inducible nitric oxide synthase expression. J Immunol 162:6171–6177.

Eliasson MJ, Sampei K, Mandir AS, Hurn PD, Traystman RJ, Bao J, Pieper A, Wang ZQ, Dawson TM, Snyder SH, Dawson VL. 1997. Poly(ADP-ribose) polymerase gene disruption renders mice resistant to cerebral ischemia. Nat Med 3:1089–1095.

Epstein AC, Gleadle JM, McNeill LA, Hewitson KS, O'Rourke J, Mole DR, Mukherji M, Metzen E, Wilson MI, Dhanda A, Tian YM, Masson N, Hamilton DL, Jaakkola P, Barstead R, Hodgkin J, Maxwell PH, Pugh CW, Schofield CJ, Ratcliffe PJ. 2001. *C. elegans* EGL-9 and mammalian homologs define a family of dioxygenases that regulate HIF by prolyl hydroxylation. Cell 107:43–54.

Fandrey J, Frede S, Jelkmann W. 1994. Role of hydrogen peroxide in hypoxia-induced erythropoietin production. Biochem J 303:507–510.

Flohé L, Günzler WA. 1984. Assays of glutathione peroxidase. Methods Enzymol 105:114–121.

Flohé L, Ötting F. 1984. Superoxide dismutase assays. Methods Enzymol 105:93–104.

Freret T, Valable S, Chazalviel L, Saulnier R, Mackenzie ET, Petit E, Bernaudin M, Boulouard M, Schumann-

Bard P. 2006. Delayed administration of deferoxamine reduces brain damage and promotes functional recovery after transient focal cerebral ischemia in the rat. Eur J Neurosci 23:1757–1765.

Garayoa M, Martínez A, Lee S, Pío R, An WG, Neckers L, Trepel J, Montuenga LM, Ryan H, Johnson R, Gassmann M, Cuttitta F. 2000. Hypoxia-inducible factor-1 (HIF-1) up-regulates adrenomedullin expression in human tumor cell lines during oxygen deprivation: a possible promotion mechanism of carcinogenesis. Mol Endocrinol 14:848–862.

Gleadle JM, Ratcliffe PJ. 1998. Hypoxia and the regulation of physiologically relevant gene expression. Mol Med Today 4:122–129.

Grisham MB, Jourd'Heuil D, Wink DA. 1999. Nitric oxide. I. Physiological chemistry of nitric oxide and its metabolites:implications in inflammation. Am J Physiol 276: G315–G321.

Groenendaal F, Shadid M, McGowan JE, Mishra OP, van Bel F. 2000. Effects of deferoxamine, a chelator of free iron, on NA(+), K(+)-ATPase activity of cortical brain cell membrane during early reperfusion after hypoxia-ischemia in newborn lambs. Pediatr Res 48: 560–564.

Habig WH, Pabst MJ, Jakoby WB. 1974. Glutathione *S*-transferases. J Biol Chem 249:7130–7139.

Hagen T, Taylor CT, Lam F, Moncada S. 2003. Redistribution of intracellular oxygen in hypoxia by nitric oxide: effect on HIF1alpha. Science 302:1975–1978.

Huang LE, Arany Z, Livingston DM, Bunn HF. 1996. Activation of hypoxia-inducible transcription factor depends primarily upon redox-sensitive stabilization of its alpha subunit. J Biol Chem 271:32253–32259.

Hurn PD, Koehler RC, Blizzard KK, Traystman RJ. 1995. Deferoxamine reduces early metabolic failure associated with severe cerebral ischemic acidosis in dogs. Stroke 26: 688–695.

Kadikoylu G, Bolaman Z, Demir S, Balkaya M, Akalin N, Enli Y. 2004. The effects of desferrioxamine on cisplatin-induced lipid peroxidation and the activities of antioxidant enzymes in rat kidneys. Hum Exp Toxicol 23:29–34.

Kietzmann T, Fandrey J, Acker H. 2000. Oxygen radicals as messengers in oxygen-dependent gene expression. News Physiol Sci 15:202–208.

Kohl R, Zhou J, Brune B. 2006. Reactive oxygen species attenuate nitric-oxide-mediated hypoxia-inducible factor-1alpha stabilization. Free Radic Biol Med 40: 1430–1442.

López-Ramos JC, Martínez-Romero R, Molina F, Cañuelo A, Martí-nez-Lara E, Siles E, Peinado MA. 2005. Evidence of a decrease in nitric oxide-storage molecules following acute hypoxia and/or hypobaria, by means of chemiluminescence analysis. Nitric Oxide 13:62–67.

Martin-Oliva D, Aguilar-Quesada R, O'valle F, Munoz-Gamez JA, Martinez-Romero R, Garcia Del Moral R, Ruiz de Almodovar JM, Villuendas R, Piris MA, Oliver FJ. 2006. Inhibition of poly(ADP-ribose) polymerase modulates tumor-related gene expression, including hypoxia-inducible factor-1 activation, during skin carcinogenesis. Cancer Res 66:5744–5756.

Metzen E, Berchner-Pfannschmidt U, Stengel P, Marxsen JH, Stolze I, Klinger M, Huang WQ, Wotzlaw C, Hellwig-Burgel T, Jelkmann W, Acker H, Fandrey J. 2003a. Intracellular localisation of human HIF-1 alpha hydroxylases: Implications for oxygen sensing. J Cell Sci 116:1319–1326.

Metzen E, Zhou J, Jelkmann W, Fandrey J, Brune B. 2003b. Nitric oxide impairs normoxic degradation of HIF-1alpha by inhibition of prolyl hydroxylases. Mol Biol Cell 14:3470–34781.

Mu D, Chang YS, Vexler ZS, Ferriero DM. 2005. Hypoxia-inducible factor 1alpha and erythropoietin upregulation with deferoxamine salvage after neonatal stroke. Exp Neurol 195:407–415.

Oliver FJ, Menissier-de Murcia J, Nacci C, Decker P, Andriantsitohaina R, Muller S, de la Rubia G, Stoclet JC, de Murcia G. 1999. Resistance to endotoxic shock as a consequence of defective NF-kappaB activation in poly (ADP-ribose) polymerase-1 deficient mice. EMBO J 18:4446–4454.

Palmer C, Roberts RL, Bero C. 1994. Deferoxamine posttreatment reduces ischemic brain injury in neonatal rats. Stroke 25:1039–1045.

Palmer LA, Semenza GL, Stoler MH, Johns RA. 1998. Hypoxia induces type II NOS gene expression in pulmonary artery endothelial cells via HIF-. Am J Physiol 274:L212–L219.

Quintero M, Brennan PA, Thomas GJ, Moncada S. 2006. Nitric oxide is a factor in the stabilization of hypoxia-inducible factor-1alpha in cancer: role of free radical formation. Cancer Res 66:770–774.

Ravati A, Ahlemeyer B, Becker A, Krieglstein J. 2000. Preconditioning-induced neuroprotection is mediated by reactive oxygen species. Brain Res 866:23–32.

Saad SY, Najjar TA, Al Rikabi AC. 2001. The preventive role of deferoxamine against acute doxorubicin-induced cardiac, renal and hepatic toxicity in rats. Pharmacol Res 43:211–218.

Schreck R, Rieber P, Baeuerle PA. 1991. Reactive oxygen intermediates as apparently widely used messengers in the activation of the NF-kappa B transcription factor and HIV-1. EMBO J 10:2247–2258.

Semenza GL. 2005. New insights into nNOS regulation of vascular homeostasis. J Clin Invest 115:3128–3139.

Seo GS, Lee SH, Choi SC, Choi EY, Oh HM, Choi EJ, Park DS, Kim SW, Kim TH, Nah YH, Kim S, Kim SH, You SH, Jun CD. 2006. Iron chelator induces THP-1 cell differentiation potentially by modulating intracellular glutathione levels. Free Radic Biol Med 40:1502–1512.

Siles E, Martinez-Lara E, Núñez MI, Muñoz-Gámez JA, Martín-Oliva D, Valenzuela MT, Peinado MA, Ruiz de Almodóvar JM, Oliver FJ. 2005. PARP-1-dependent 3-nitrotyrosine protein modification after DNA damage. J Cell Biochem 96:709–715.

Siren AL, Fratelli M, Brines M, Goemans C, Casagrande S, Lewczuk P, Keenan S, Gleiter C, Pasquali C, Capobianco A, Mennini T, Heumann R, Cerami A, Ehrenreich H, Ghezzi P. 2000. Erythropoetin prevents neuronal apoptosis after cerebral ischemia and metabolic stress. Proc Natl Acad Sci USA 98:4044–4049.

Sogawa K, Numayama-Tsuruta K, Ema M, Abe M, Abe H, Fujii-Kuriyama Y. 1998. Inhibition of hypoxia-inducible factor 1 activity by nitric oxide donors in hypoxia. Proc Natl Acad Sci USA 95:7368–7373.

Wang GL, Jiang BH, Rue EA, Semenza GL. 1995. Hypoxia-inducible factor 1 is a basic-helix-loop-helix-PAS

heterodimer regulated by cellular O_2 tension. Proc Natl Acad Sci USA 92:5510–5514.

Wang M, Kirk JS, Venkataraman S, Domann FE, Zhang HJ, Schafer FQ, Flanagan SW, Weydert CJ, Spitz DR, Buettner GR, Oberley LW. 2005. Manganese superoxide dismutase suppresses hypoxic induction of hypoxia-inducible factor-1alpha and vascular endothelial growth factor. Oncogene 24:8154–8166.

Weiss G, Werner-Felmayer G, Werner ER, Grunewald K, Wachter H, Hentze MW. 1994. Iron regulates nitric oxide synthase activity by controlling nuclear transcription. J Exp Med 180:969–976.

Williams RE, Zweier JL, Flaherty JT. 1991. Treatment with deferoxamine during ischemia improves functional and metabolic recovery and reduces reperfusion-induced oxygen radical generation in rabbit hearts. Circulation 83:1006–1014.

Woo KJ, Lee TJ, Park JW, Kwon TK. 2006. Desferrioxamine, an iron chelator, enhances HIF-1alpha accumulation via cyclooxygenase-2 signalling pathway. Biochem Biophys Res Commun 343:8–14.

Yang ZZ, Zhang AY, Yi FX, Li PL, Zou AP. 2003. Redox regulation of HIF-1alpha levels and HO-1 expression in renal medullary interstitial cells. Am J Physiol Renal Physiol 284:F1207–F1215.

Zaman K, Ryu H, Hall D, O'Donovan K, Lin KI, Miller MP, Marquis JC, Baraban JM, Semenza GL, Ratan RR. 1999. Protection from oxidative stress-induced apoptosis in cortical neuronal cultures by iron chelators is associated with enhanced DNA binding of hypoxia inducible factor-1 and ATF-1/CREB and increased expression of glycolytic enzymes, p21WAF1/cip1, and erythropoetin. J Neurosci 19:9821–9830.

Zhang Z, Ren J, Harlos K, McKinnon CH, Clifton IJ, Schofield CJ. 2002. Crystal structure of a clavaminate synthase-Fe(II)-2-oxoglutarate-substrate-NO complex: evidence for metal centered rearrangements. FEBS Lett 517:7–12.

Zhou HZ, Swanson RA, Simonis U, Ma X, Cecchini G, Gray MO. 2006. Poly(ADP-ribose) polymerase-1 hyperactivation and impairment of mitochondrial respiratory chain complex I function in reperfused mouse hearts. Am J Physiol Heart Circ Physiol 29:H714–H723.

Zhu H, Bunn HF. 1999. Oxygen sensing and signaling: impact on the regulation of physiologically relevant genes. Respir Physiol 115:239–247.

Zingarelli B, Cuzzocrea S, Zsengeller Z, Salzman AL, Szabo C. 1997. Protection against myocardial ischemia and reperfusion injury by 3-aminobenzamide, an inhibitor of poly (ADP-ribose) synthetase. Cardiovasc Res 36:205–215.

Zingarelli B, O'Connor M, Hake PW. 2003. Inhibitors of poly(ADP-ribose) polymerase modulate signal transduction pathways in colitis. Eur J Pharmacol 469:183–194.